

招待論文
Invited Paper

Invited Paper

PRESENT STATUS AND FUTURE APPROACH OF TURBULENCE MODELING

By Ching Jen CHEN* and Shenq Yuh JAW**

The paper discusses the state-of-the-art of turbulence modeling and presents possible ways for improvement in the future turbulence models. Based on a set of turbulence closure postulations, a variation of second-order turbulence models, such as the Reynolds stress model (RSM), the algebraic stress model ($k-\epsilon-A$), and the eddy viscosity model ($k-\epsilon-E$), are obtained. Examples of prediction made are free shear flows, cavity flows, and flows past an off-set channel. Although a complete turbulence model does not exist at the present time, some prediction capability has been achieved by the second-order turbulence model. The incompleteness of turbulence modeling may be attributed to the inadequacy of isotropic dissipation and single turbulent scale postulations. Use of multiple turbulence scale concepts, including use of fractal dimension of turbulent eddies may improve turbulence prediction.

Keywords : turbulence modeling, multiple scale, fractal, Reynolds stress, $k-\epsilon$ model

1. INTRODUCTION

Complex turbulent flows exist in many circumstances in our natural environment, as well as in man-made and industrial environments. For example, turbulent flows occur in oceans, in rivers, in atmosphere, and even in the lungs of a human being. On the other hand, turbulent flows also occur in flying an airplane, driving a car, heating and cooling of a house, burning of gas and coal in furnaces, and blood flow past prosthetic heart valves. Although the Navier-Stokes equation can properly describe the details of turbulent motions, it is too costly and often time consuming for engineers and physicists to solve such a complex and detailed solution. Instead, ensemble averaged Navier-Stokes equations are often sufficient and practical to describe the turbulent motions confronting engineering and physical problems. However, in taking an average of the Navier-Stokes equations for the turbulent flow which is three-dimensional, unsteady, random, irregular, and rotational, detailed information of fluid motions are lost in the averaging process. In order to recover the information lost during the averaging process, a turbulence model must be introduced. However, no such unified turbulence model is available at the present time although some prediction capability has been achieved by turbulence modeling. The objective of the present paper is to discuss the state-of-art of turbulence modeling and to present possible ways for improvement in the future turbulence model. Without a unified turbulence model that is capable of predicting the averaged turbulent flows, our understanding of turbulence phenomena will remain incomplete and hamper engineering design.

* Professor and Chairman, Department of Mechanical Engineering, Senior Research Engineer, Iowa Institute of Hydraulic Research, The University of Iowa (Iowa City, Iowa 52242)

** Research Assistant, Department of Mechanical Engineering, The University of Iowa (Iowa City, Iowa 52242)

2. VISCOUS FLUID MODEL

The historical development of turbulence modeling can be mirrored to the historical development of viscous fluid modeling. The mathematical modeling of fluid motion was advanced from the continuum, inviscid fluid model when the Euler equation was derived in 1755, to the viscous conducting fluid model known as the Navier-Stokes equations proposed first by Navier in 1823 and later by Stokes in 1845. It took almost a century of effort by many scientists, mathematicians, physicists, and engineers to develop the Navier-Stokes viscous fluid model. The Navier-Stokes equations describe viscous fluid motion so well that it is often now forgotten that the Navier-Stokes equations are a model for viscous fluid motion.

The postulations made by Navier and Stokes for the derivation of the viscous fluid model have a strong bearing on the modeling of turbulent flows. These postulations, known as the Stokes Principle, can be summarized and rephrased as follows :

- ① Fluid can be considered to be continuum. Molecular motions are averaged and thus detailed information on the dynamics of molecular collision is lost. A model is required to recover the lost information (modeling requirement).
- ② The diffusion of momentum by viscous fluid motion is proportional to the rate of deformation (diffusion gradient model).
- ③ Fluid is assumed to be isotropic (isotropic molecular collision model).
- ④ Fluid is assumed to be homogeneous.
- ⑤ When fluid is at rest, the viscous stress is the hydrostatic pressure (consistency and realizability requirement).
- ⑥ When the flow is of a pure dilatation, the average viscous stress is equal to the pressure (Stokes hypothesis).
- ⑦ Viscous fluid model moduli (density and viscosity) require experimental calibration and determinations (uniqueness of moduli).

The postulation that fluid is continuum eliminates the need of the description about the intermolecular forces and collision. In order to recover the lost information on the molecular collision due to the continuum postulation, a viscous fluid model must be introduced and the model modulus, such as viscosity, must be calibrated by performing experiments. The same is true when an averaging is imposed on the Navier-Stokes equations for turbulent motion, the details of turbulent motions are eliminated. In order to recover the lost information during the averaging process, a turbulence model must be introduced and turbulence model moduli must be determined from experiments. It should be remarked that the Navier-Stokes equation is not restricted to laminar fluid motion and should be perfectly capable of describing the turbulent fluid motion. The turbulent flow motion predicted by directly solving the Navier-Stokes equations is known as the direct simulation.

3. TURBULENCE MODEL

It has been almost one century, since Reynolds introduced in 1895 the time averaged Navier-Stokes equations, that researchers and scientists have attempted to create a turbulence model for Reynolds stresses to recover the lost information of turbulent motion in the averaging process. In the early 20th century, due to lack of computing machines, turbulence models were restricted to be relatively simple and intuitive. These models are very limited in the sense that the model can apply only to a particular problem or problems with similar geometry and is inappropriate for predicting other types of flow or geometry. An example of such a model is known as the mixing length theory proposed by Prandtl in 1925. These simple models, in general, have low prediction capabilities. However, they have the advantage of simplicity and are capable of modeling turbulence with similar flow conditions and geometry shapes.

With the advances of high speed computing after World War II, turbulence modeling also advances.

From the late 1950's until the present time, turbulence modeling in engineering practice has progressed to the second order turbulence closure model in which the second order turbulence transport equations, namely, Reynolds stress equations, turbulent kinetic energy equation, and rate of dissipation of turbulent kinetic energy are modelled to a close set of equations. At the present time, there are many second order turbulence models available. These are reviewed by Chen¹⁾ and Lakshminarayana²⁾. Many variations of the second order turbulence closure models are available. The prediction capability of the second order closure model has greatly improved over that of the simple turbulence model. Chen and Singh³⁾ extracted the basic postulations that are adopted by most turbulence models at the present time. These postulations can be analogously formulated after the Stokes principles for the viscous fluid model. They are summarized below.

- ① Ensemble averaged Navier-Stokes equations can properly describe turbulent mean motion and turbulent transport properties. Instantaneous fluid motions are averaged and detailed information of fluid motions is lost. A model is required to recover the lost information (modeling requirement).
- ② The diffusion of turbulent transport properties by turbulence is proportional to the gradient of transport properties (diffusion gradient model).
- ③ Small turbulent eddies are isotropic (isotropic dissipation model).
- ④ All turbulence transport quantities are local functions of Reynolds stress, turbulence kinetic energy, rate of dissipation turbulent kinetic energy, mean flow variables, and thermodynamics variables ($\overline{u_i u_j}$, k , ε , U_i , ρ , P , T) (one point correlation closure statement).
- ⑤ All modelled turbulent phenomenon must be consistent in symmetry, invariance, permutation, and physical observations (consistency and realizability requirement).
- ⑥ Turbulent phenomenon can be characterized by one turbulent scale based on turbulent kinetic energy and its rate of dissipation (k , ε) (turbulence scale hypothesis).
- ⑦ All turbulence model moduli require experimental calibration and determination (uniqueness of moduli).

It should be remarked that if a turbulence model is complete, then the turbulence model moduli are unique and invariant to turbulent flow conditions and geometry. However, at the present time, no such turbulence model is available. Therefore, many variations of turbulence models, and hence model moduli, under the above postulations, are in existence, such as a high Reynolds number turbulence model^{4),5)}, low Reynolds number turbulence model^{6),7)}, near wall turbulence model⁸⁾, two-scale turbulence model⁹⁾, etc. Some models made an adhoc adjustment while some models attempted to relax the above postulations. For example, to modify postulations 3 and 6, one may consider that small turbulent eddies are anisotropic to replace postulation 3, and that the turbulence phenomenon requires multiple scale to replace postulation 6.

4. THE REYNOLDS STRESS MODEL

Based on the postulations made for the turbulence model, one may obtain a variation of second order turbulence models. One of the popular second order turbulence models was proposed by Hanjalic and Launder⁴⁾ for incompressible fluid which is summarized and compared with the exact equations below. Ensemble averaged incompressible Navier-Stokes Equations are

$$\frac{\partial U_i}{\partial X_i} = 0 \dots\dots\dots (1)$$

$$\left. \begin{aligned} \rho \frac{DU_i}{Dt} &= \rho G_i - \frac{\partial p}{\partial X_i} + \frac{\partial \tau_{ij}}{\partial X_j} + \frac{\partial \tau_{ij}^t}{\partial X_j} \\ \tau_{ij} &= \mu \left(\frac{\partial U_i}{\partial X_j} + \frac{\partial U_j}{\partial X_i} \right), \quad \tau_{ij}^t = -\rho \overline{u_i u_j} \end{aligned} \right\} \dots\dots\dots (2)$$

Here the viscous stress τ_{ij} is modelled from the viscous fluid model (Stokes Principle) and the Reynolds stress τ_{ij}^t is modelled from the turbulence model (Turbulence Closure Postulations).

Exact $\overline{u_i u_j}$ Equation

$$\frac{D\overline{u_i u_j}}{Dt} = D_{ij} + P_{ij} - \varepsilon_{ij} + \Phi_{i,j,1} + \Phi_{i,j,2}$$

or

$$\begin{aligned} \frac{D\overline{u_i u_j}}{Dt} = \frac{\partial}{\partial X_i} \left[-\overline{u_i u_j u_i} - \frac{p}{\rho} (\delta_{ji} u_i + \delta_{ii} u_j) + \nu \frac{\partial \overline{u_i u_j}}{\partial X_i} \right] \\ - \left(\overline{u_i u_i} \frac{\partial U_j}{\partial X_i} + \overline{u_j u_i} \frac{\partial U_i}{\partial X_i} \right) - 2\nu \frac{\partial u_i}{\partial X_i} \frac{\partial u_j}{\partial X_i} + \frac{p}{\rho} \left[\frac{\partial u_i}{\partial X_j} + \frac{\partial u_j}{\partial X_i} \right] \dots \dots \dots (3 E) \end{aligned}$$

Modelled $\overline{u_i u_j}$ Equation ($C_k=0.09\sim 0.11$, $C_1=2.3\sim 2.8$, $C_2=0.4\sim 0.6$)

$$\begin{aligned} \frac{D\overline{u_i u_j}}{Dt} = \frac{\partial}{\partial X_i} \left[C_k \frac{k^2}{\varepsilon} \frac{\partial \overline{u_i u_j}}{\partial X_i} + \nu \frac{\partial \overline{u_i u_j}}{\partial X_i} \right] - \left(\overline{u_i u_i} \frac{\partial U_j}{\partial X_i} + \overline{u_j u_i} \frac{\partial U_i}{\partial X_i} \right) \\ - \frac{2}{3} \delta_{ij} \varepsilon - C_1 \frac{\varepsilon}{k} \left(\overline{u_i u_j} - \frac{2}{3} \delta_{ij} k \right) \\ + C_2 \left(\overline{u_i u_i} \frac{\partial U_j}{\partial X_i} + \overline{u_j u_i} \frac{\partial U_i}{\partial X_i} - \frac{2}{3} \delta_{ij} \overline{u_n u_m} \frac{\partial U_n}{\partial X_m} \right) \dots \dots \dots (3 M) \end{aligned}$$

Exact k Equation

$$\frac{Dk}{Dt} = D_k + P_k - \varepsilon \quad (k = \overline{u_i u_i}/2, \quad k' = u_i u_i/2)$$

or

$$\frac{Dk}{Dt} = \frac{\partial}{\partial X_i} \left[-\overline{u_i} \left(k' + \frac{p}{\rho} \right) + \nu \frac{\partial k}{\partial X_i} \right] - \overline{u_i u_i} \frac{\partial U_i}{\partial X_i} - \varepsilon \dots \dots \dots (4 E)$$

Modelled k Equation ($C_k=0.09\sim 0.11$)

$$\frac{Dk}{Dt} = \frac{\partial}{\partial X_i} \left[C_k \frac{k^2}{\varepsilon} \frac{\partial k}{\partial X_i} + \nu \frac{\partial k}{\partial X_i} \right] - \overline{u_i u_i} \frac{\partial U_i}{\partial X_i} - \varepsilon \dots \dots \dots (4 M)$$

Exact ε Equation ($\varepsilon = \nu \frac{\partial u_i}{\partial X_i} \frac{\partial u_i}{\partial X_i}$, $\varepsilon' = \nu \frac{\partial u_i}{\partial X_i} \frac{\partial u_i}{\partial X_i}$)

$$\frac{D\varepsilon}{Dt} = D_\varepsilon + P_{\varepsilon_1} + P_{\varepsilon_2} - P_{\varepsilon_3} - DS$$

or

$$\begin{aligned} \frac{D\varepsilon}{Dt} = \frac{\partial}{\partial X_i} \left[-\left(\overline{u_i \varepsilon'} + \frac{2\nu}{\rho} \frac{\partial u_i}{\partial X_j} \frac{\partial p}{\partial X_j} \right) + \nu \frac{\partial \varepsilon}{\partial X_i} \right] \\ - 2\nu \frac{\partial U_i}{\partial X_j} \left[\frac{\partial u_i}{\partial X_i} \frac{\partial u_i}{\partial X_j} + \frac{\partial u_i}{\partial X_i} \frac{\partial u_j}{\partial X_i} \right] - 2\nu u_i \frac{\partial u_i}{\partial X_j} \frac{\partial^2 U_i}{\partial X_i \partial X_j} \\ - 2\nu \frac{\partial u_i}{\partial X_j} \frac{\partial u_i}{\partial X_i} \frac{\partial u_j}{\partial X_i} - 2 \left(\nu \frac{\partial^2 u_i}{\partial X_i \partial X_j} \right)^2 \dots \dots \dots (5 E) \end{aligned}$$

Modelled ε Equation ($C_\varepsilon=0.07$, $C_{\varepsilon_1}=1.42\sim 1.45$, $C_{\varepsilon_2}=1.90\sim 1.92$)

$$\frac{D\varepsilon}{Dt} = \frac{\partial}{\partial X_i} \left[C_\varepsilon \frac{k^2}{\varepsilon} \frac{\partial \varepsilon}{\partial X_i} + \nu \frac{\partial \varepsilon}{\partial X_i} \right] - C_{\varepsilon_1} \frac{\varepsilon}{k} \overline{u_i u_j} \frac{\partial U_j}{\partial X_i} - C_{\varepsilon_2} \frac{\varepsilon^2}{k} \dots \dots \dots (5 M)$$

The turbulence model, such as shown above, is known⁹ as the Reynolds Stress Model (RSM) since it models the Reynolds stress transport equation, as well as k and ε equations. In principle, the above Reynolds stress model or a variation of it^{9,10} is closed in the sense that it has the same number of equations for the number of unknown variables U_i , p , $\overline{u_i u_j}$, k , and ε . The six model moduli C_k , C_1 , C_2 , C_ε , C_{ε_1} , and C_{ε_2} are determined and calibrated from experimental measurements of several fundamental flows, mostly from flows of air. Details of determination for this moduli are given from experiments and summarized by Chen¹¹. Briefly C_{ε_2} is determined from isotropic grid turbulent flow¹¹, C_1 from anisotropic grid turbulent flow with an area concentration 4 : 1¹², C_2 and C_{ε_1} from two dimensional homogeneous shear

flow¹³, C_ϵ from turbulent boundary layer flow in the constant turbulent kinetic energy region¹⁴, and C_k from oscillating grid turbulence¹⁵. It should be remarked that all these moduli are determined from flow of air except the last moduli, C_k , which is calibrated from experiments with water. The general view on these moduli is that since they are dimensionless, these moduli should be also applicable to other fluids. Although the model moduli can be, in general, a dimensionless function of $\overline{u_i u_j}$, k , ϵ , U_i , ρ , P , and T , they are found to be mostly constants and often referred to as turbulence model constants. It should be remarked here that a slight adjustment of these moduli is in popular use. For example, experimental determination for C_k is 0.23 while $C_k=0.09$ is often used. Also, experimental determination of C_ϵ is 0.04 while $C_\epsilon=0.07$ is often used. The most deviation for turbulence moduli is C_{ϵ_1} which from experimental determination should be close to C_{ϵ_2} or $C_{\epsilon_1} \doteq C_{\epsilon_2} = 1.92$. However, $C_{\epsilon_1} = 1.45$ is often a necessary value if one is to avoid enormous error in the prediction. The need for modifying the turbulence moduli indicates the imperfection of the state of turbulence modeling. Nevertheless, the second order turbulence model is still the most convenient and practical model for engineering solutions today.

5. TWO-EQUATION APPROXIMATION ($k-\epsilon$ MODEL)

In principle, the above Reynolds stress model (RSM) is complete to model the averaged turbulent flows. However, it often requires much effort to solve these equations.

(1) Algebraic stress model ($k-\epsilon-A$ model)

As a compromise, the quantities k and ϵ are solved from differential transport equations while the Reynolds stresses $\overline{u_i u_j}$ are solved from the approximated algebraic equations. Rodi^{16,17} proposed to modify the Reynolds stress equation (3) by assuming that

$$\text{(Convection-Diffusion) of } \overline{u_i u_j} = \frac{\overline{u_i u_j}}{k} (P_k - \epsilon) \dots \dots \dots (6)$$

This expression assumes that $\overline{u_i u_j}$ vary in proportion to the kinetic turbulent energy. By combining Eqs. (3M) and (6), the algebraic expression for $\overline{u_i u_j}$ becomes

$$\overline{u_i u_j} = k \left[\frac{\frac{2}{3} (C_1 - 1) \epsilon \delta_{ij} + (1 - C_2) P_{ij} + \frac{2}{3} C_2 P_k \delta_{ij}}{\epsilon C_1 + (P_k - \epsilon)} \right] \dots \dots \dots (7)$$

When Reynolds stress equation (3) in the RSM turbulence model is replaced by Eq. (7), the turbulence model is called the $k-\epsilon-A$ model. A simpler version of $k-\epsilon-A$ model is the equilibrium $k-\epsilon-A$ model when $(P_k - \epsilon)$ in the denominator of Eq. (7) is set equal to zero. Many researchers used even simpler turbulence models. One of them is the $k-\epsilon-E$ model.

(2) $k-\epsilon$ -Eddy viscosity model ($k-\epsilon-E$ model)

Boussinesq in 1877¹⁸ proposed that the turbulent stresses are, analogously to the viscous stresses, proportional to velocity gradients with an eddy viscosity ν_t as the proportional constant. The generalization of Boussinesq's eddy viscosity model is

$$-\overline{u_i u_j} = \nu_t \left(\frac{\partial U_i}{\partial X_j} + \frac{\partial U_j}{\partial X_i} \right) - \frac{2}{3} \delta_{ij} k \dots \dots \dots (8)$$

Based on dimensional analysis of k and ϵ , ν_t is defined as $\nu_t = C_\mu k^2 / \epsilon$. k and ϵ are governed by Eqs. (4) and (5), respectively. $C_\mu = 0.09$ is a constant determined from experiments. When Eq. (8) is used to replace Eq. (3), the turbulence model is called the $k-\epsilon-E$ model or the standard $k-\epsilon$ model¹⁶. At present, the $k-\epsilon-E$ model is one of the most widely used turbulence models. The $k-\epsilon-E$ model is based on Boussinesq's adhoc assumption and is considered less rigorous than the $k-\epsilon-A$ model. The constant, C_μ , which is defined in Eq. (8) has been calibrated by many experimental data to be approximately 0.09. Rodi¹⁷ studied many experimental measurements and found that C_μ is equal to 0.09 only when a flow is in local equilibrium, i.e., $P_k = \epsilon$.

Modification for C_μ and other turbulent moduli such as C_{ϵ_1} and C_{ϵ_2} are thus suggested and made¹⁶ in

order to effectively use the $k-\epsilon-E$ model for prediction of turbulent flows.

6. ACHIEVEMENT AND WEAKNESS OF THE TURBULENCE MODEL

The Reynolds Stress Model (RSM) provided above contains only six turbulence model moduli or constants. One way to provide a critical test of the accuracy of the RSM is to eliminate or minimize the gravitational force, pressure gradient, and viscous stress in Eq. (2) that affecting the turbulent flow so that the development of the flow field is dominated by the Reynolds stress $\overline{u_i u_j}$ which is modelled. Incompressible free shear flow, such as plane jet, round jet, wake flows and mixing layers, are good benchmark tests for the turbulence model since at fairly large Reynolds number flow the right-hand side of Eq. (2) is dominated only by the Reynolds stress term.

Hanjalic and Launder⁴⁾ were the first to apply the RSM to predict plane jet flow and plane mixing layer flow and compute U , k , ϵ , and $\overline{u\overline{v}}$ from the equations (2), (3M), (4M), and (5M) except that $\overline{v^2}$ is replaced with the empirical measurement $\overline{v^2}=0.5 k$. The predicted behavior of mean velocity, turbulent kinetic energy, and Reynolds stress are generally in satisfactory accord. As an example, Fig. 1 shows the results for plane jet in stagnant ambient. Most importantly, the predicted rates of spread in plane jet and plane mixing layer were satisfactory. However, they have not attempted the prediction of round jet or axisymmetric wake. Recently, Jaw¹⁹⁾ studied the prediction of the RSM for the round jet and found that, as shown in Fig. 2, the RSM substantially over predicted the spreading rate and Reynolds stress of the round jet. The Reynolds stress turbulence model, as it is, still has difficulty in predicting simple flow. Therefore, any attempt to improve the turbulence model must first demonstrate that the improved model is capable of accurately predicting the two dimensional as well as axisymmetric jet and wake flows. No RSM turbulence model at the present time has clearly been shown to predict satisfactorily for the flows mentioned.

Examining the postulations made in deriving the turbulence model, we find that postulations 3 and 6 seem to be too restrictive and too simplistic. Postulation of isotropic dissipation leads to the omission of $P_{\epsilon 1}$,

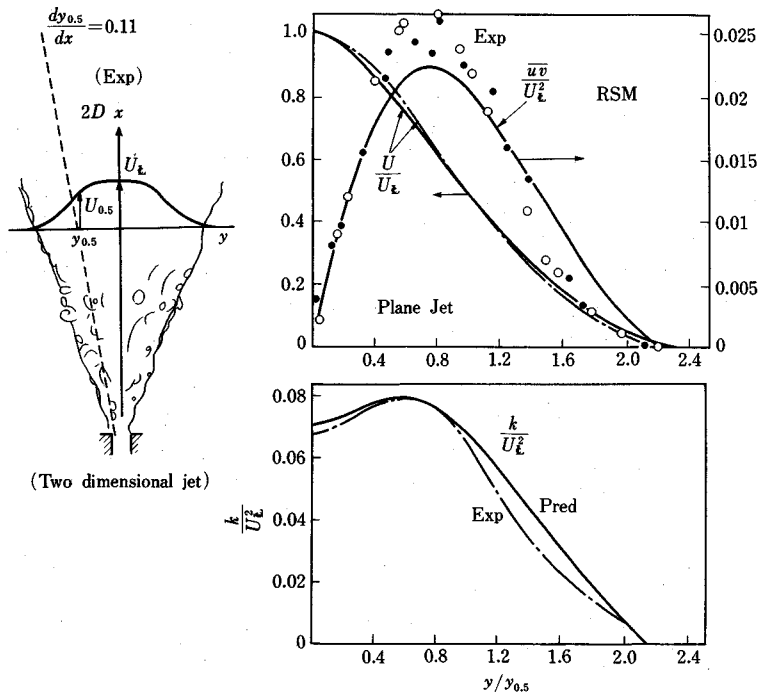
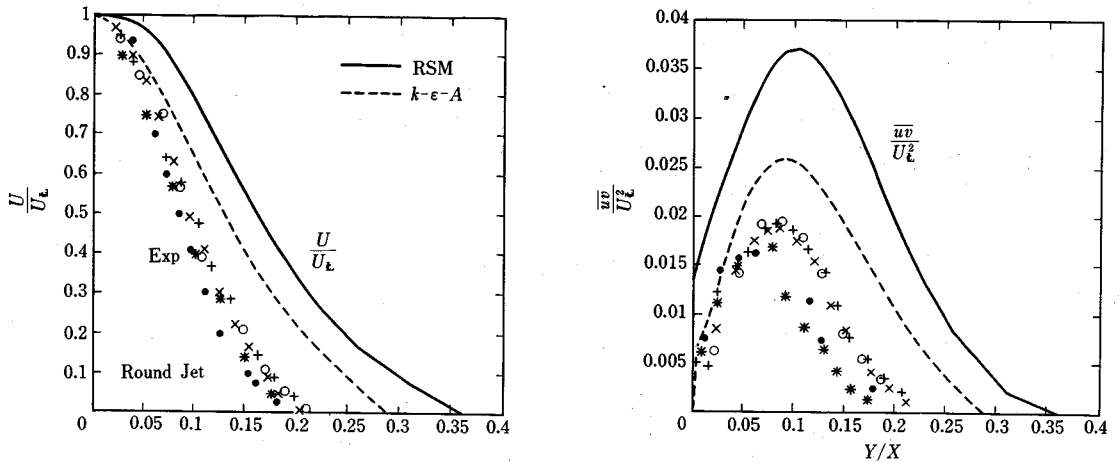


Fig.1 RSM Prediction of Plane Jet Flow.

Fig. 2 RSM and $k-\epsilon-A$ Prediction of Round Jet Flow.

the production term due to interaction between mean flow and dissipating eddies in Eq. (5 E). Postulation 6 assumes that the turbulent flow can be characterized by one turbulence scale based on (k, ϵ) from the energy containing eddies. That has led us to believe the turbulence time scale is $t \sim k/\epsilon$. This time scale is employed by Lumley^{20, 21)} to model the last two terms of ϵ equation by setting $P_{\epsilon 3} - DS \doteq \left[\frac{1}{t} \right] (P_k - \epsilon) \doteq \frac{\epsilon}{k} (C_{\epsilon 1} P_k - C_{\epsilon 2} \epsilon)$. All these may contribute to the necessity of adjusting $C_{\epsilon 1}$ value in Eq. (5 M) from a value close to $C_{\epsilon 2} = 1.92$ to $1.42 \sim 1.45$ and many studies show that both $C_{\epsilon 1}$ and $C_{\epsilon 2}$ must be modified with a correction function. It should be also remarked here that while most turbulent predictions and calculations are not as sensitive, as they should be, to small variations of moduli $C_k, C_1, C_2,$ and C_ϵ , many computations are quite sensitive to small variations of $C_{\epsilon 1}$ and $C_{\epsilon 2}$. Three significant digits for $C_{\epsilon 1}$ and $C_{\epsilon 2}$ must generally be specified if a stable result of computation is expected. This symptom leads to the current thinking that a multiple scale is necessary to make fundamental progress in turbulence modeling.

While the turbulence model for predicting free shear flows is only partially successful, Hanjalic and Launder⁵⁾ and Launder, Reece, Rodi⁹⁾ showed that the RSM turbulence model predicts better for wall boundary layer and wall jet flows and more satisfactory asymmetric channel flow with different roughness of the wall and symmetric annular flow.

Rodi^{16, 17)} demonstrated the capability of the $k-\epsilon-E$ model in predicting many free shear flows including plane and axisymmetric jet, plane and axisymmetric wake, and mixing layer flow. Chen¹⁾ showed that the $k-\epsilon-E$ model and the $k-\epsilon-A$ model for free shear flow, where large gradients of velocity and transport properties are confined to a small layer, is essentially the same. While the $k-\epsilon-E$ or $k-\epsilon-A$ model with $C_k = 0.09, C_\epsilon = 0.07, C_{\epsilon 1} = 1.44, C_{\epsilon 2} = 1.92$ and $C_\mu = 0.09$, is capable of satisfactory prediction for many flows, they also suffered the same difficulties as the RSM in predicting axisymmetric jet (see Fig. 2) and wake flows poorly. Rodi¹⁷⁾, in an attempt to improve the $k-\epsilon-E$ model, found from empirical calibration that if C_μ is made to be a function of the ratio of turbulent energy production to its dissipation rate, P/ϵ , the $k-\epsilon-E$ model can be made to predict reasonably satisfactorily for many free shear flows.

There are many modifications proposed for the Reynolds stress model and the $k-\epsilon$ model when they are applied to different problems such as near wall flow^{22)~24)}, curved flow^{25), 26)}, swirling flow²⁾, strongly anisotropic flow²⁷⁾, and low Reynolds number flow^{6), 7), 28)}. Many modifications consider the turbulence moduli to be a function of local turbulent Reynolds numbers, the distance from the boundary, and anisotropic behavior. A good survey and review of these modification are given by Rodi^{16), 27), 29)}, Patel *et al.*²⁶⁾, Launder and Shima³⁰⁾, Martinuzzi and Pollard³¹⁾, Hanjalac³²⁾, Shima²³⁾, and Bernard²⁴⁾.

7. COMPARISON OF MODELS

(1) Reynolds stress model and $k-\epsilon-E$ model

Ushijima *et al.*³³⁾ performed a detailed experimental measurement of an offset channel ($520 \times 450 \times 100$ mm) flow shown in Fig. 3 and compared the measurements to predictions from three turbulent models, namely the SRSM (Simple Reynolds Stress Model) of Eqs. (3 M), (4 M) and (5 M), the $k-\epsilon-E$ model with Eq. (8) replacing Eqs. (3 M), and the modified RSM model or LRSM (Launder Reynolds Stress Model¹⁹⁾) where D_{ij} , D_k , D_ϵ , and $\Phi_{ij,2}$ in Eqs. (3 E), (4 E), and (5 E) are replaced and modelled by

$$D_{ij} = \frac{\partial}{\partial X_m} \left[C_s \frac{K}{\epsilon} \left(\overline{u_i u_j} \frac{\partial \overline{u_m}}{\partial X_i} + \overline{u_j u_i} \frac{\partial \overline{u_m}}{\partial X_i} + \overline{u_m u_i} \frac{\partial \overline{u_j}}{\partial X_i} \right) \right]$$

$$D_k = \frac{\partial}{\partial X_m} \left[C_s \frac{K}{\epsilon} \left(\overline{u_i u_n} \frac{\partial \overline{u_i u_m}}{\partial X_n} + \overline{u_m u_n} \frac{\partial \overline{u_i}}{\partial X_n} \right) + \nu \frac{\partial k}{\partial x_m} \right]$$

$$D_\epsilon = \frac{\partial}{\partial X_m} \left[C'_\epsilon \frac{K}{\epsilon} \overline{u_i u_j} \frac{\partial \epsilon}{\partial X_n} + \frac{\partial \epsilon}{\partial x_m} \right], \quad Q_{ij} = - \left(\overline{u_i u_m} \frac{\partial U_m}{\partial X_j} + \overline{u_j u_m} \frac{\partial U_m}{\partial X_i} \right)$$

$$\Phi_{ij,2} = - \left[\frac{(C_2 + 8)}{11} (P_{ij} - \frac{2}{3} P_{\kappa} \delta_{ij}) + \frac{(30 C_2 - 2)}{55} k \left(\frac{\partial U_i}{\partial X_j} + \frac{\partial U_j}{\partial X_i} \right) + \frac{(8 C_2 - 2)}{11} \left(Q_{ij} - \frac{2}{3} P_{\kappa} \delta_{ij} \right) \right]$$

with $C_s=0.11$ and $C'_\epsilon=0.15$, $C_1=1.5$, $C_2=0.4$, $C_{\epsilon 1}=1.44$ and $C_{\epsilon 2}=1.90$.

With the Reynolds number, based on inlet channel height (50 mm) and velocity (20 cm/sec), 10^4 , the velocity and turbulent transport properties are computed by the above three turbulence models. The prediction of the flow near the wall is replaced by the near wall functions¹⁾. The near wall functions are introduced to account for the anisotropic behavior of turbulence near the wall which is not properly modelled and to avoid the computation effort needed at the near wall zone where the velocity and turbulent transport properties vary rapidly. Derivations of wall function are given by Ushijima *et al.*³³⁾ or Chen¹⁾.

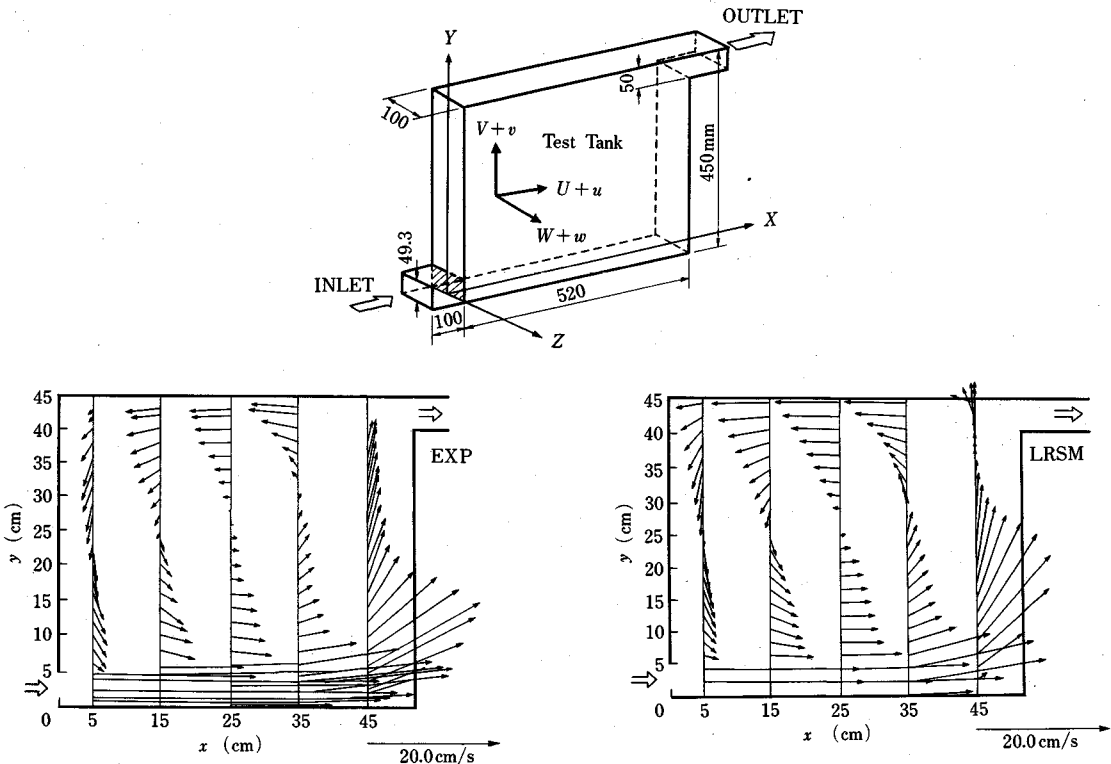


Fig. 3 Offset Channel Flow and Velocity Vector.

$$u^+ = U/U^* = 5.67 \ln U^* X_n / \nu,$$

$$\nu_t = C_w (C_\mu k^2 / \varepsilon) = C_w k^* X_n U^*, \quad C_w = 3.0, \quad k^* = 0.4, \quad C_\mu = 0.09$$

$$k = 3.6 U^{*2}, \quad \varepsilon = \frac{U^{*3}}{k^* X_n}, \quad U^* = \left(\frac{\tau_w}{\rho} \right)^{1/2}$$

$$\overline{u^2} = 6.2 U^{*2}, \quad \overline{v^2} = \overline{w^2} = 0.53 U^{*2}, \quad -\overline{uv} = \pm 0.046 U^{*2}, \quad \overline{vw} = \overline{uw} = 0$$

Some of the predicted results are shown in Figs. 3 and 4. All three models predicted reasonably for the mean velocity, U , except near the wall. Slightly more discrepancies are found for the turbulent transport variables, $\overline{u^2}$, $\overline{v^2}$, and \overline{uv} than the prediction of mean velocity. Again, more deviation is found near the wall. In an overall comparison, the simple Reynolds stress model, SRMS, predicts slightly better than the k - ε - E and LRMS models. Walter and Chen⁽³⁾ performed flow visualization of the same offset channel flow at $Re = 4 \times 10^3$, with a scaled down (by a factor of 4.5) experiment and confirmed the overall flow pattern in the chamber.

The above example illustrates the present status of turbulence models in predicting turbulent flows.

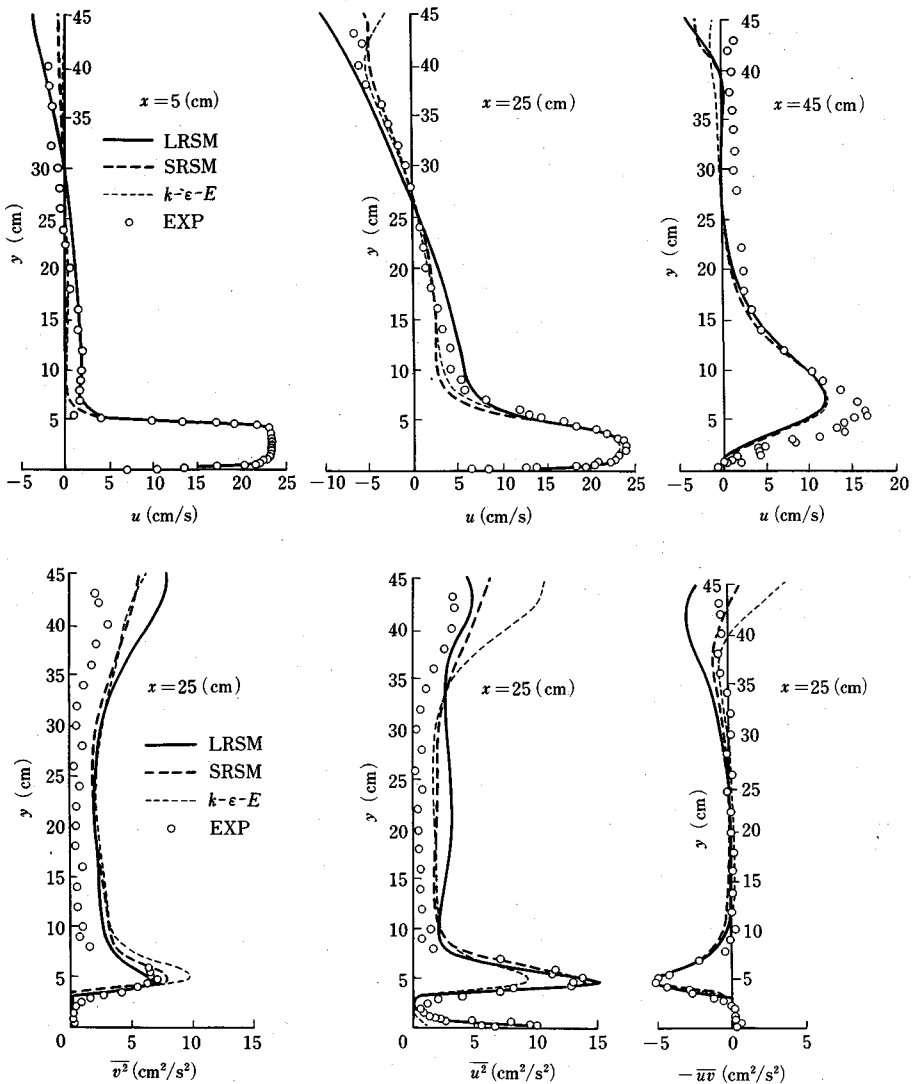


Fig. 4 Comparison of Velocity Profiles and Reynolds Stresses.

Obviously, some prediction capability has been established. However, the turbulence model is still not perfect, particularly the turbulent behavior near the wall. This may be again traced back mainly to the inadequacy of the postulations 3 and 6 in which the small turbulent eddies are assumed to be isotropic such that ε_{ij} is modelled as $2\varepsilon\delta_{ij}/3$ and the turbulence is characterized with one scale based on (k, ε) . The near wall turbulent behavior or low turbulent Reynolds number region evidently cannot be properly described with isotropic dissipation and one scale hypothesis. Turbulence modeling with an anisotropic dissipation and multiple scale concept may provide some fundamental improvement in prediction of turbulent phenomena. It should also be remarked that the turbulence model postulation 5, the consistency and realizability requirement, has not been completely met by most of the turbulence models in use.

(2) k - ε - E model and k - ε - A model

Before we discuss ideas for future improvement, let us examine the more approximate turbulence models, namely the k - ε - A and k - ε - E models. The two models are generally known as the k - ε model or two equation model because only two differential equations for k and ε are used in modeling the turbulent transport properties. In general the two models are different. The k - ε - A model has a more complex expression for the Reynolds stresses including the anisotropic diffusion effect. It was shown, however, by Chen¹⁾ that in the boundary-layer-like flow the k - ε - A and k - ε - E moduli are essentially identical. Therefore, in order to compare the difference between the two models, we consider recirculating flow in cavity here.

The k - ε - E model is also known as the standard k - ε model²⁷⁾ and the k - ε - A model is also known as the algebraic stress model. Using the near wall functions, Chen and Chang³⁵⁾ compared the prediction of the k - ε - E model and the k - ε - A model with the experimental measurements of Mills³⁶⁾, Girard and Curlet³⁷⁾, Grand³⁸⁾ and Normandin³⁹⁾ for driven square and rectangular cavity (1 : 3 ratio) flows.

Fig. 5 is a plot of the mean velocity U , V and $\overline{v^2}$ along the centerline of driven square cavity flow³⁶⁾ at Reynolds number of 4.8×10^5 . The line with 0 is the prediction of the k - ε - E model and \square is that of the k - ε - A model. The experimental data are denoted by + and Δ . In general, the prediction agrees well with the experimental data. The predictions of U and V by the k - ε - A model are almost identical to those by the k - ε - E model. In the central region, both models slightly underpredict the magnitude of the mean velocity. It is noted that Grand's data³⁸⁾ is closer to the predicted results than data of Girard and Curlet³⁷⁾ in the central region. Fig. 5 also shows the distribution of V velocity and the Reynolds normal stress $(\overline{v^2})^{1/2}$ along the horizontal centerline of the cavity. It is seen that the stress is the largest near the right wall where the fluid just leaves the driven wall and turns upward. The normal stress, $\overline{v^2}$, is also predicted to be larger near the wall than that at the center, but the left-hand side is only about two-thirds as large as that of the right wall. The reason that larger stress occurs near the wall is because the mean velocity gradients near wall regions are larger. Thus, it is expected to produce more turbulence near the wall. In general, the k - ε - A model predicts larger normal stress, $\overline{v^2}$, than the k - ε - E model does.

Fig. 6 shows the predictions of the rectangular cavity flow with an aspect ratio of 3 and a Reynolds number of 200 000. The prediction of the mean velocity V on the horizontal centerline H-F is compared with Normandin's experimental data³⁹⁾. In general, the comparison is good except that the predicted magnitudes near the wall are slightly smaller than the experimental data. Comparison of the predicted and measured Reynolds stress $(\overline{v^2})^{1/2}$ shows that the experimental data are substantially higher than the predicted values. Chen and Chang³⁵⁾ found that the prediction of mean velocity by the two models is approximately the same. However, the normal Reynolds stresses predicted by the k - ε - A model shows more variation than those predicted by the k - ε - E model.

The above examples show again that some prediction capability by the k - ε - E and k - ε - A models is accomplished, particularly the mean velocity distribution for engineering purposes. One reason for more success in prediction recirculating flow is that the convection in such flow is affected not only the Reynolds stress but also the pressure gradient and viscous stress. Therefore the turbulent flow prediction becomes

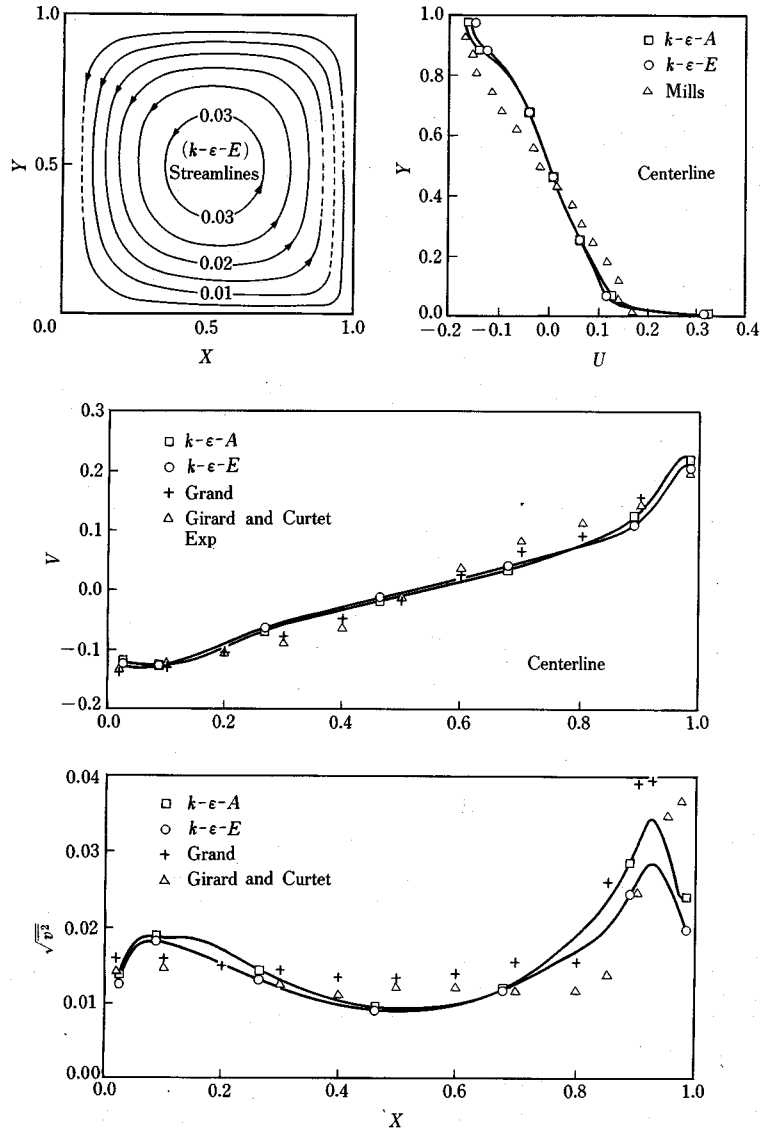


Fig.5 $k-\epsilon$ Model Prediction of Driven Square Cavity Flow.

less sensitive to the accuracy of the turbulence model even though the flow may appear to be complex. However, the prediction of Reynolds stress, especially near the wall, is far from perfect. The use of the near wall function certainly is not adequate and is one of the major contributors to the discrepancies between the prediction and the experiment.

(3) Wall function method and zonal model

Recently, attempts⁽⁴⁰⁾⁻⁽⁴²⁾ have been made to remove the use of near wall function in the calculation of wall shear flows. This is prompted by realizing that, first, the near wall function is inaccurate particularly when there exists a large pressure gradient⁽²⁹⁾, and second, the near wall function cannot be easily specified when there is a separation or the flow is near the reattaching point. With the availability of computing power, one may be tempted to carry the calculation all the way to the wall with the RSM or $k-\epsilon$ model since it then eliminates the need of wall function for the mean velocity and turbulent transport properties. However, one soon will find that such solution is not only inaccurate, but above all, very unstable. It is

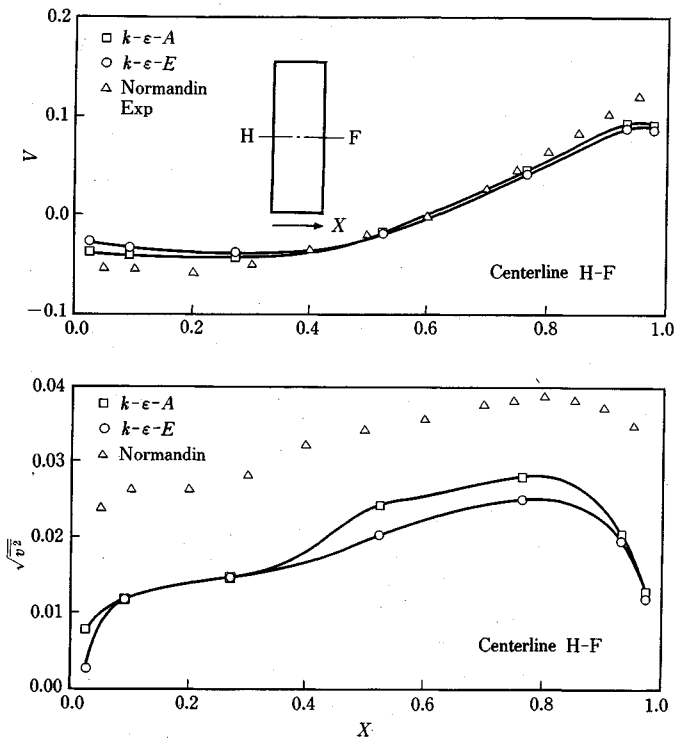


Fig. 6 $k-\epsilon$ Model Prediction of Driven Rectangular Cavity Flow.

found that the ϵ equation is most unstable even with the use of the correction function for $C_{\epsilon 1}$ and $C_{\epsilon 2}$. Thus, the zone model approach was conceived. The basic idea of zonal modeling is to carry the calculation to the wall with, at the present status, the $k-\epsilon$ model, except the near wall zone where, approximately y^+ up to 100, the dissipation rate of turbulent kinetic energy, ϵ , and the turbulent eddy viscosity, ν_t , are specified by algebraic equations which may more adequately model the near wall proximity of viscous effects and anisotropy of turbulence. The outer region is the rest of the computational region. The $k-\epsilon-E$ turbulence model is used to simulate the turbulent outer region.

Examples of zonal turbulence models are the Hassid and Poreh model⁽⁴³⁾, the Norris and Reynolds model⁽⁴⁴⁾, and the Wolfshtein model⁽⁴⁵⁾. Choi and Chen⁽⁴²⁾ compared the wall function method and the Wolfshtein zonal model in predicting turbulent flow past an axisymmetric body. In the Wolfshtein zonal turbulence model, the turbulent eddy viscosity, ν_t , and the rate of turbulent kinetic energy dissipation, ϵ , in the near wall region is specified by a simple algebraic form

$\epsilon = k^{3/2}/l_\epsilon$, $\nu_t = C_\mu k^{1/2} l_\mu$. The length scales, l_ϵ and l_μ , are considered to be functions of viscosity in the near wall region in terms of turbulence Reynolds number R_k . Wolfshtein proposed⁽⁴⁵⁾

$$l_\mu = By [1 - \exp(-R_k/A_\mu)], \quad l_\epsilon = By [1 - \exp(-R_k/A_\epsilon)]$$

$$R_k = Rey k^{1/2}, \quad C_\mu = 0.09, \quad B = k^* c_\mu^{-3/4}, \quad A_\epsilon = 2B, \quad A_\mu = 70$$

where y is the normal distance from the wall, and k^* is the Karman constant. The constants, A_ϵ and A_μ , in the above equations are reevaluated by Chen and Patel⁽⁴¹⁾ and are slightly different from those reported in Wolfshtein⁽⁴⁵⁾. Choi and Chen⁽⁴²⁾ computed the flow past AFTERBODY 1, an axisymmetric body with both the wall function method and zonal model. Fig. 7 shows that although the $k-\epsilon-E$ model with wall function predicted the surface pressure coefficient, C_p , and the mean velocity profiles, U and V , approximately the same as the zonal model, it predicted much worse than the zonal model for the turbulent kinetic energy, particularly near the tail of the body and in the wake zone. Choi and Chen⁽⁴²⁾ also demonstrated an important improvement that the zonal model may predict the reverse flow when the wall function method fails.

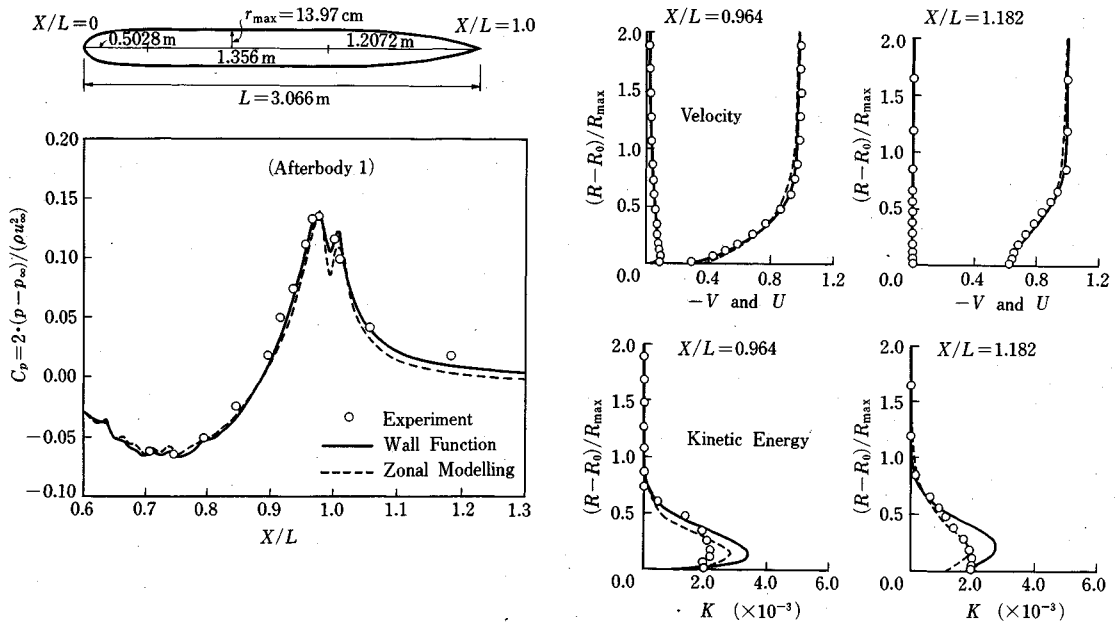


Fig. 7 Comparison of Zonal Model and Wall Function.

8. MULTIPLE SCALE TURBULENCE MODEL

Many attempts have been made in recent years to improve the predictability of the second order turbulence model. Some of the models adopt the multiple scales in the turbulence modeling. One of early attempts was proposed by Hanjalic *et al.*⁴⁶⁾. They attributed the incorrect prediction for some turbulent flows to the use of a single-time-scale in the turbulence modeling. They reasoned that turbulence is comprised of fluctuating motions with a spectrum of sizes and time scales. Since different turbulent interactions are known to be associated with different parts of the spectrum, the idea that one can mimic the response of the Reynolds stresses with a mathematical model containing just one time scale seems highly simplistic. Although numerous successful applications of single-time-scale models have been reported in the literature, this may be due to the flows considered having been fairly close to a spectral equilibrium where the single-time-scale hypothesis is adequate. On the other hand, there are a few applications where the present one scale turbulence model fails, as pointed out earlier. Therefore, Hanjalic *et al.*⁴⁶⁾ proposed a simple multiple-time-scale model by dividing the whole energy spectrum into two parts—the energy containing eddies and the energy dissipating eddies. Separate transport equations are solved for the turbulence energy across the spectrum. Conceptually, the multiple-time-scale model is expected to be superior to the single-time-scale model in predicting shear flows not in local equilibrium. The application of the two-time-scale turbulence model, proposed by Hanjalic⁴⁶⁾, showed some improvement in predicting round jet.

Wilcox⁴⁷⁾ began with the premise that turbulence can be described by representing the turbulence energy spectrum in terms of an upper and a lower partition. The upper partition corresponds to the lowest frequency, energy-bearing eddies which are more or less inviscid. Eddies in the lower partition are expected to contain most of the vorticity which is isotropic, and dissipative. Wilcox thus postulated that the lower partition of the spectrum is responsible for the equilibrium value of the Reynolds-stress tensor, whereas the upper partition gives rise to departure from equilibrium.

From these postulations Wilcox⁴⁷⁾ obtained a two equation model⁴⁸⁾ and an additional inviscid tensor equation for the upper partition contribution to the Reynolds-stress tensor. A feature of the Wilcox model

is that it uses a single turbulence-length-scale determining equation. This model has been successfully applied to several different turbulent flows including homogeneous turbulence, two-dimensional boundary layers, and unsteady boundary layers including periodic separation and reattachment. However, the model has not demonstrated that it is capable of predicting plane and axisymmetric jet or plane and axisymmetric wake flow.

Instead of using the idea of dividing energy spectrum, Chen and Singh³⁾ proposed a two-scale model by adopting both the large eddy or energy-containing scale (k , ϵ) and the small eddy or energy dissipation scale (ϵ , ν) in the turbulence modeling, where ν is the kinematic viscosity of the fluid. The second scale is based on the well known Kolmogorov hypothesis that dissipation of turbulent kinetic energy occurs primarily at small eddies.

The experiments of Friche *et al.*⁴⁹⁾ reveal that large eddies possess most of the turbulent kinetic energy in the flow and do not play any significant role in the dissipation of turbulent kinetic energy. On the other hand, Kolmogorov⁵⁰⁾ found that characteristics of small eddies are function of (ϵ , ν). Chen and Singh³⁾ in addition reasoned that an eddy provides a mechanism to transfer the turbulent kinetic energy possessed by large eddies to small eddies before it is consumed by the viscous dissipation and turned into thermal energy. Hence, it seems natural to consider both turbulence scales in the turbulence modeling.

The concept of using both (k , ϵ) and (ϵ , ν) scales was first proposed by Lumley²⁰⁾. He suggested that each term in both the k and ϵ equations be modelled either by using the (k , ϵ) scales or the (k , ϵ , ν) scales. However, in the final form of the modelled ϵ -equation suggested by Lumley, the scale containing ν was neglected. Chen and Singh³⁾, on the other hand, used both the (k , ϵ) and (ϵ , ν) scales in the modeling of the k and ϵ equation. They considered the Kolmogorov scale (ϵ , ν) should be used for the dissipation or destruction term of the k and ϵ equations. Since the exact expression of ϵ appears as the dissipation in the k equation, no modeling is required. For the ϵ equation, Chen and Singh modelled the last two terms of the ϵ equation according to Lumley's assumption²⁰⁾, $P_{\epsilon 3} - DS = \left[\frac{1}{t} \right] (P_k - \epsilon)$, but invoking the Kolmogorov time scale $[t] = (\nu/\epsilon)^{1/2}$ for it in the modeling. They considered that other turbulent diffusion and production terms are modelled by the (k - ϵ) scale as before. By recalibration of the new two scale ϵ and k equations with the same experimental data used before they gave

$$C_k = 0.9, \quad C'_\epsilon = 2.00, \quad C_{\epsilon 1} = 17.5 Re^{-1/2}, \quad C_{\epsilon 2} = 18.7 Re^{-1/2}$$

in place of C_ϵ , $C_{\epsilon 1}$, and $C_{\epsilon 2}$. Re is the Reynolds number based on the large characteristic length scale and mean velocity. Then Chen and Singh demonstrated that the two scale k - ϵ - E model predicted satisfactorily the spreading rate for many free shear flows including round and plane jet, plane wake, mixing layer and buoyant plane and round jet. Fig. 8 shows the comparison of the one scale and two scale k - ϵ - E model with experimental data for plane and round jet.

9. DIRECT SIMULATION AND TURBULENCE MODEL

Parallel with the achievements in engineering application of the use of turbulence models, the advent of supercomputers and new numerical algorithms made it possible to perform direct simulation of turbulent flows at moderate Reynolds numbers. The attraction of direct simulation is that it eliminates the need for the adhoc model. These simulations can be used to compute the terms in the budget of the Reynolds stresses. It is then possible to test the turbulence closure models by direct comparison of the closure formula with the direct computation of the term being modelled. In the future approach to turbulence modeling, the data computed from direct simulation can be used as a guided and numerical benchmark. Mansour and Shih⁵¹⁾ reviewed the most recent advances in direct simulation and turbulence modeling.

Rogallo^{52), 53)} provided data for homogeneous turbulence where he computed the terms in the budget of the Reynolds stress. Recently, Reynolds stress budgets in flows with inhomogeneity in one direction were computed by Moser and Moin⁵⁴⁾ in a curved channel, Spalart^{55), 56)} of a flow over a flat plate, and Mansour, Kim, and Moin²²⁾ in a channel flow. The budgets for homogeneous flows were computed at higher

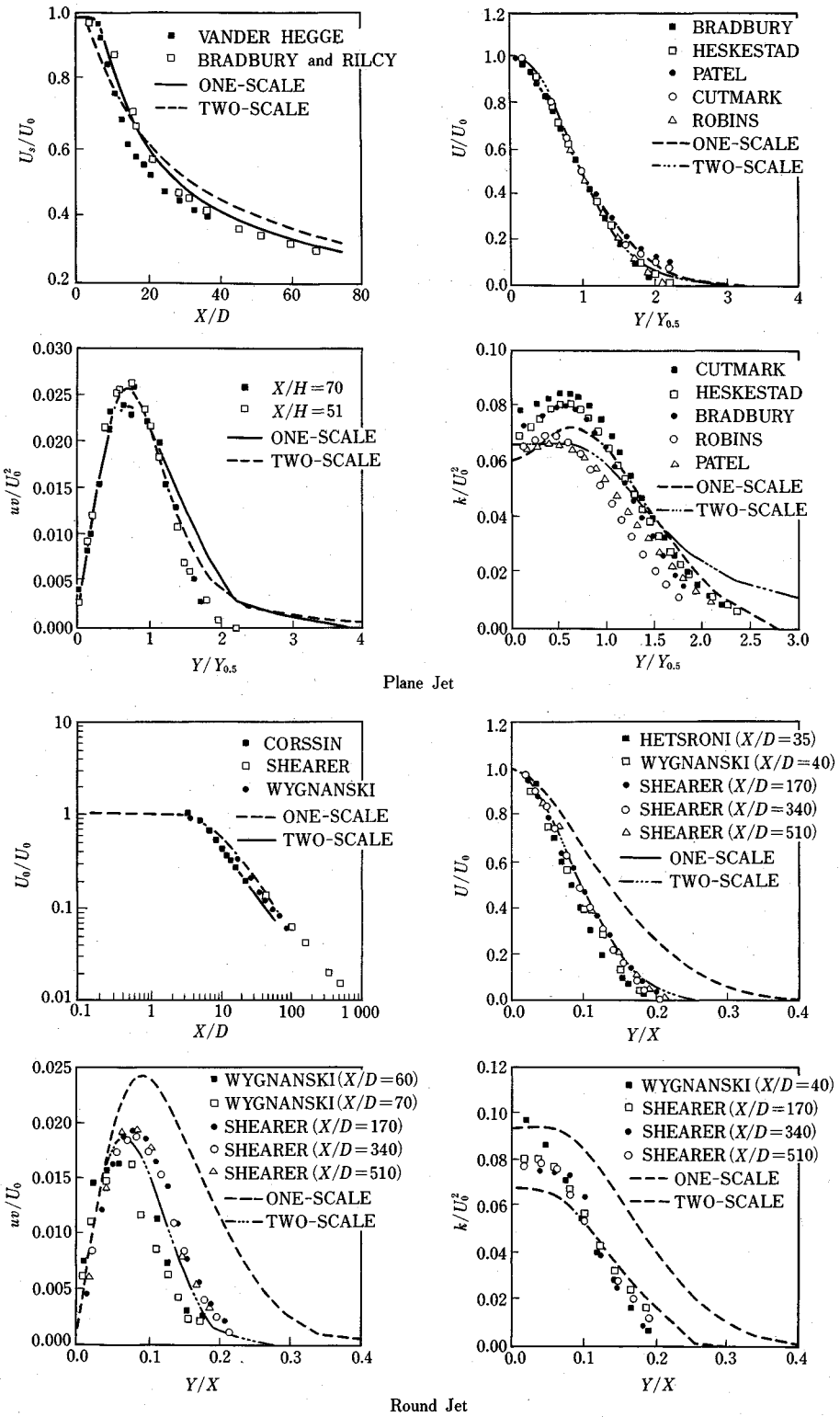


Fig. 8 Comparison of One Scale and Two Scale $k-\epsilon$ Model.

resolutions than the original work of Rogallo by Lee and Reynolds⁵⁷⁾ for homogeneous flows under irrotational strain, and by Rogers, Moin and Reynolds⁵⁸⁾ for homogeneous flows under mean shear.

An example is the comparison between the direct simulation and various turbulence models. Mansour, Kim and Moin²²⁾ showed that the dissipation term, ε_{ij} , in the $\overline{u_i u_j}$ equation, Eq. (3 E), is better modelled as $\varepsilon_{ij} = \overline{u_i u_j} \varepsilon / k$ than $\varepsilon_{ij} = 2 \varepsilon \delta_{ij} / 3$ and that the simpler modeling of $-\overline{u_i u_j u_i}$ in Eq. (3 E) as

$$-\overline{u_i u_j u_k} = C'_s \frac{k \overline{u_i u_j}}{\varepsilon} \frac{\partial}{\partial X_i} (\overline{u_i u_j})$$

performs better than that proposed by LRSM⁹⁾ and used by Ushijima *et al.*³³⁾

10. FRACTALS IN TURBULENCE MODELING

In the previous section, multiple scale concept in turbulence modeling was discussed. Many proposals^{3), 46), 48)} in incorporating multiple scale have been made. They all seem to improve some aspect of turbulence modeling. The success of multiple scale in turbulence modeling depends on the understanding of one or more scales, other than that of (k, ε) , that accurately reflects the turbulent manifestation of turbulent eddies in carrying out dissipation, diffusion and redistribution. Recent development of the fractal concept may eventually be useful in turbulence modeling.

The neologism fractal appeared about 24 years ago when Mandelbrot in 1967⁵⁹⁾ introduced the term "fractal" to describe the behavior of a rocky coastline. He found that the length of the coastline had a power-law dependence on the length of the measuring stick. The power defined the fractal dimension. Subsequently, Mandelbrot⁶⁰⁾ associated many physical processes and mathematical constructions with fractal behavior.

Several different, supposedly more precise, definitions of fractal dimension are now found in the literature. In the most basic sense, fractals are objects that display self-similarity over a wide range of scales. Analogous to the Euclidean dimension of classical objects, each fractal object, or turbulent eddy, is associated with a characteristic dimension called the fractal dimension which forms a basic measure of its fragmentation or roughness. The fractal dimension has the property of being strictly greater than the object's topological dimension. Mathematically, the fractal dimension D is defined as $D = \log N / \log (1/E)$ which is essentially an exponent that characterizes self-similarity of the object under study. The object is made of N parts, each of which is obtained from the whole by a reduction of ratio E .

In 1922, Richardson⁶¹⁾ thought that fully-developed turbulence consisted of a hierarchy of eddies, or scales of various orders. It is this description of turbulent flows, namely that they are "objects" consisting of a hierarchy of scales, that leads to the expectation that the theory of fractals must be applicable to turbulence. Indeed, evidence of a connection between fractals and turbulent flows is found from a study of the structure of turbulent eddies observed in flow visualization experiments⁶²⁾ and from similar arguments from classical turbulence theory or numerical simulation of turbulent flow⁶³⁾.

Fractal dimensions of several types of turbulent flow have been determined by Screenivasan and Meneveau⁶⁴⁾, e.g., regions of active dissipation, turbulent/non-turbulent interface of boundary layer flow, axisymmetric jet, plane wake, mixing layer, etc. However, it is not clear how, given the dimensions for several of its facets, one can solve the inverse problem of reconstructing the original set. If fractals are to be applied to turbulence closure problems, this question must be addressed.

One possible way to incorporate fractals in turbulence modeling is to adopt the intermittency model, β model, presented by Frisch *et al.*⁶⁵⁾. The key assumption of the Frisch model is that the small-scale structures of turbulence become less and less space filling as the scale size decreases. Consider a discrete sequence of scales or "eddies", $l_n = l_0 2^{-n}$, $n=0, 1, 2, \dots$ if the largest eddies, l_0 , are space filling, after n generations only a fraction $\beta_n = \beta^n = (N/2^3)^n$ of the space will be occupied by active fluid, where N is the average number of eddies formed by each eddy of the proceeding generation and is related to the fractal dimension D by $N = 2^D$; $N \leq 8$. For instance, let v_n denote a typical velocity difference over a distance $\sim l_n$

in an active region, then the kinetic energy per unit mass on scales $\sim l_n$ is given by $k_n \sim \beta_n \nu_n^2$.

By introducing a simple dynamical argument, Frisch *et al.*⁽⁶⁵⁾ obtained the following relationships

$$\nu_n \sim \varepsilon^{1/3} l_n^{1/3} (l_n/l_0)^{-1/3(3-D)}$$

$$t_n \sim \varepsilon^{-1/3} l_n^{2/3} (l_n/l_0)^{(3-D)/3}$$

$$k_n \sim \varepsilon^{2/3} l_n^{2/3} (l_n/l_0)^{(3-D)/3}$$

where t_n is the eddy turnover time, ε is the energy dissipation rate.

From these relationships, we can derive new turbulent scales, including the fractal dimension D , as

$$l = \left[\frac{k^{3(D-3)}}{\nu^{-3} \varepsilon^{-2+D}} \right]^{\frac{1}{1+D}}, \quad t = \left[\frac{k^{3(D-3)}}{\nu^{D-5} \varepsilon^{2D-4}} \right]^{\frac{1}{1+D}}$$

Note that when D is equal to 3, then $l = (\nu^3/\varepsilon)^{1/4}$, $t = (\nu/\varepsilon)^{1/2}$, which is the classical dissipation scale, the Kolmogorov scale⁽⁵⁰⁾, we have mentioned earlier. However, Screenivasan and Meneveau⁽⁶⁴⁾ showed from experimental observation that the fractal dimension of dissipative structures of turbulence is $D \approx 2.7$. The new turbulent scales, with $D \approx 2.7$, may imply that a reasonable intermediate turbulent scale, between the energy containing large scale (k , ε) and Kolmogorov microscale (ν , ε), has been found. Although at present the fractal has not been used in the turbulence model, the multiple scale utilizing the fractal scale may improve the behavior of the existing turbulence models. Furthermore, the elliptical fractals⁽⁶⁶⁾⁻⁽⁶⁸⁾ may be used to modify the anisotropic turbulence model. All of those are under investigation by the authors.

11. CONCLUSION

The modern development of turbulence modeling began in the 1940's and '50's, and the applications of second order turbulence modeling began in 1960 when computing machines became available to handle the computation required using the advanced turbulence models. In the 1970's, the application of the k - ε model became very popular, however, most of the calculations were two-dimensional in nature. In the 1980's, the computation has been extended to three-dimensional problems and the use of more advanced turbulence models, many of which use Reynolds stress models. Although there are other approaches to turbulence modeling such as large eddy simulations or sub-grid modeling, the most popular trend at the present time and in the foreseeable future, is the Reynolds stress model and its simplified version of the k - ε model. The availability of numerical results from direct simulation of turbulent flow is one of the important advances in turbulence modeling. Since many of the high order correlations are difficult to obtain from experimental measurement which has hampered the progress of turbulence modeling. Although the direct simulation by direct computation of the Navier-Stokes equations may eventually find its way into engineering applications, such an approach largely depends on the availability of supercomputing machines. It is perhaps safe to say that in the next ten years, engineering solutions to turbulent flow problems may rely heavily on turbulence modeling of Reynolds stress equations.

ACKNOWLEDGEMENTS

This research is in part supported by the Naval AHR Grant N00167-86-k-0019 administered by the Office of Naval Research.

REFERENCES

- 1) Chen, C.J. : Prediction of Turbulent Flows, CRIEPI (Central Research Institute of Electric Power Industry), Tech. Report 17, Abiko, Japan, November 1983.
- 2) Lakshminarayana, B. : Turbulent Modeling for Complex Shear Flows, AIAA Journal, Vol. 24, No. 12, pp.1900-1917, 1986.
- 3) Chen, C.J. and Singh, K. : Prediction of Buoyant Free Shear Flows by k - ε Model Based on Two Turbulence Scale Concept, Proceedings International Symposium on Buoyant Flows, Athens, Greece, 1-5 September, 1986, pp.26-36. Also IIHR Report No. 299, Iowa Institute of Hydraulic Research, The University of Iowa, Iowa City, Iowa, October 1986.
- 4) Hanjalic, K. and Launder, B.E. : A Reynolds-Stress Model of Turbulence and Its Application to Thin Shear Flows, Journal of Fluid Mechanics, Vol. 52, pp.609-638, 1972.

- 5) Hanjalic, K. and Launder, B. E. : Contribution Towards a Reynolds-Stress Closure for Low-Reynolds-Number Turbulence, *Journal of Fluid Mechanics*, Vol. 74, pp.593-610, 1976.
- 6) So, R.M.C. and Yoo, G. J. : Low Reynolds Number Modeling of Turbulent Flows with and without Wall Transpiration, *AIAA Journal*, Vol. 25, No.12, pp. 1556-1564, 1987.
- 7) Jones, W.P. and Launder, B. E. : The Calculation of Low Reynolds-Number Phenomena with a Two-Equation Model of Turbulence, *Int. J. Heat Mass Transfer*, Vol. 10, pp.1119-1130, 1973.
- 8) Launder, B. E. and Reynolds, W. C. : Asymptotic Near-Wall Stress Dissipation Rates in a Turbulent Flow, *Physics of Fluids*, Vol. 26, pp. 1157-1158, 1983.
- 9) Launder, B. E., Reece, G. J. and Rodi, W. : Progress in the Development of a Reynolds-Stress Turbulence Closure, *Journal of Fluid Mechanics*, Vol. 68, pp. 537-566, 1975.
- 10) Kline, S. J., Cantwell, B. and Lilley, G. M. (eds.) : *Complex Turbulent Flows : Comparison of Computation and Experiment*, Stanford University Press, Stanford, CA, 1982.
- 11) Batchelor, G.K. and Townsend, A. A. : Decay of Vorticity in Isotropic Turbulence, *Proceedings Roy. Soc., A* 190, pp. 534-550, 1947.
- 12) Uberoi, M. S. : Equipartition of Energy and Local Isotropy in Turbulent Flow, *Journal of Applied Physics*, Vol. 28, No. 10, pp. 1165-1170, 1957.
- 13) Champagne, F. H., Harris, V. G. and Corrsin, S. : Experiments on Nearly Homogeneous Shear Flows, *J. Fluid Mech.*, Vol. 41, pp. 81-140, 1970.
- 14) Klebanoff, P. S. : Characteristics of Turbulence in a Boundary Layer with Zero Pressure Gradient, NACA Rep. 1247, 1955.
- 15) Komatsu Toshimitsu, Matsunaga Nobuhiro, *et al.* : Defect of $k-\epsilon$ Turbulence Model and Its Improvements, *Proceedings 30 th Japan Conference on Hydraulics*, pp. 529-534, Feb. 1986.
- 16) Rodi, W. : Examples of Turbulence Models for Incompressible Flow, *AIAA Journal*, Vol. 20, pp. 872-879, 1982.
- 17) Rodi, W. : The Prediction of Free Turbulent Boundary Layers by Use of a Two-Equation Model of Turbulence, Ph. D. Dissertation, Department of Mechanical Engineering, Imperial College, University of London, 1972.
- 18) Boussinesq, J. : *Essai sur la theorie des eaux courantes*, *Mem. Acad. Sci., Paris*, 23, p. 46, 1877.
- 19) Jaw, S. Y. : Development of An Anisotropic Turbulence Model for Prediction of Complex Flows, Report, Department of Mechanical Engineering, The University of Iowa, August 1989.
- 20) Lumley, J. L. : Prediction Method for Turbulent Flows, Lecture Series 76, von Karman Institute for Fluid Dynamics, March 3-7, 1975, Rhode-St-Genese, Belgium.
- 21) Lumley, J. L. : Computational Modeling of Turbulent Flows, *Advances in Applied Mech.*, Vol. 18, pp. 123-176, 1978.
- 22) Mansour, N. N., Kim, J. and Moin, P. : Reynolds-Stress and Dissipation Rate Budgets in a Turbulent Channel Flow, *J. Fluid Mech.*, Vol. 194, pp. 15-44, Sept. 1988.
- 23) Shima, N. : A Reynolds-Stress Model for Near-Wall and Low-Reynolds-Number Regions, *Journal of Fluid Engineering*, Vol. 110, pp. 38-44, March 1988.
- 24) Bernard, P. S. : Limitations of the Near-Wall $k-\epsilon$ Turbulence Model, *AIAA Journal*, Vol. 24, No. 4, pp. 619-622, April 1986.
- 25) Park, S. W. and Chung, M. K. : Curvature-Dependent Two-Equation Model for Prediction of Turbulent Recirculating Flows, *AIAA Journal*, Vol. 27, No. 3, pp. 340-344, 1989.
- 26) Patel, V. C., Rodi, W. and Scheuerer, G. : Turbulence Models for Near-Wall and Low Reynolds Number Flow : A Review, *AIAA Journal*, Vol. 33, No. 9, pp. 1308-1318, 1985.
- 27) Rodi, W. : Recent Developments in Turbulence Modeling, *Proc. 3 rd Int'l. Sym. on Refined Flow Modeling and Turbulence Measurements*, eds. Y. Iwasa, N. Tamai, A. Wada, Tokyo, Japan, July 26-28, 1988.
- 28) Chien, K.-Y. : Predictions of Channel and Boundary-Layer Flows with a Low Reynolds Number Turbulence Model, *AIAA Journal*, Vol. 20, No. 1, pp. 33-38, 1982.
- 29) Rodi, W. : Scrutinizing the $k-\epsilon$ Turbulence Model Under Adverse Pressure Gradient Conditions, *Journal of Fluid Engineering*, Vol. 108, pp. 174-179, June 1986.
- 30) Launder, B. E. and Shima, N. : Second-Moment Closure for the Near-Wall Sublayer : Development and Application, *AIAA Journal*, Vol. 27, No. 10, pp. 1319-1325, October 1989.
- 31) Martinuzzi, R. and Pollard, A. : Comparative Study of Turbulence Models in Predicting Turbulent Pipe Flow, Part I : Algebraic Stress and $k-\epsilon$ Models, *AIAA Journal*, Vol. 27, No. 1, pp. 29-36, January 1989.
- 32) Hanjalic, K. : Practical Predictions by Two-Equation and Other Fast Methods, *Proceedings of Zoran P. Zaric Memorial International Seminar on Near-Wall Turbulence*, Dubrovnik, Yugoslavia, May 16-20, 1988, Hemisphere Publishing Corp.
- 33) Ushijima, S., Kato, M., Fujimoto, K. and Moriya, S. : Application of Some Turbulence Models-Numerical Analysis of Two-Dimensional Circulation Flows, *Civil Eng. Lab. Rep. No. 385019*, Central Research Institute of Electric Power Industry (CRIEPI), Abiko City, Chiba, Japan, September 1985.
- 34) Walter, J. A. and Chen, C. J. : Flow Visualization of Particle Streaks in Offset Channel Flow by a Direct CCD Imaging

- Process, ASME Winter Annual Meeting, Symposium on Flow Visualization IV, San Francisco, California, December 10-15, 1989 (ASME FE-5 C), FED-Vol. 85, Flow Visualization, pp. 115-120.
- 35) Chen, C. J. and Chang, S. M. : Prediction of Turbulent Flows in Rectangular Cavity with $k-\epsilon-A$ and $k-\epsilon-E$ Models, presented at 2nd International Symposium on Refined Flow Modeling and Turbulent Measurements, Sept. 16-18, Iowa City Iowa, USA, 1985, in Turbulence Measurements and Flow Modeling, ed. by Chen, C. J., Chen, L.-D., and Holly, F. M., Jr., Hemisphere Publishing Co., pp. 611-620, 1986.
 - 36) Mills, R. D. : On the Closed Motion of a Fluid in a Square Cavity, J. Royal Aeronautical Society, Vol. 69, pp. 116-120, February, 1965.
 - 37) Girard, J. and Curlet, R. : Etude Des Courants De Recirculation Dans Une Cavite, Institute De Mecanique De Grenoble, Grenoble, France, 1975.
 - 38) Grand, D. : Contribution a L'Etude des Courants de Recirculation, these de Doctorate d'Etat, Universite de Grenoble, 17 April, 1975.
 - 39) Normandin, M. : Etude Experimental de L'ecoulement Turbulent dans Une Cavite Profonde, L'Universite Scientifique Et Medicale L'Institut National Polytechnique De Grenoble, Ph. D. Thesis, Grenoble, France, 1978.
 - 40) Iacovides, H. and Launder, B. E. : PSL-An Economic Approach to the Numerical Analysis of Near-Wall, Elliptic Flow, ASME, J. Fluids Eng., Vol. 106, pp. 241-242, June 1984.
 - 41) Chen, H. C. and Patel, V. C. : Near-Wall Turbulence Models for Complex Flows Including Separation, AIAA J., Vol. 26, pp. 641-648, 1988.
 - 42) Choi, S. K. and Chen, C. J. : Finite Analytic Numerical Solution of Turbulence Flow Past Axisymmetric Bodies by Zonal Modeling Approach, ASME Winter Annual Meeting, November 28-December 2, Chicago, Illinois, 1988, and Advances and Application in Computational Fluid Dynamics, edited by Baysal, FED, Vol. 66, pp. 23-32.
 - 43) Gibson, M. M., Spalding, D. B. and Ziner, W. : Boundary-Layer Calculations Using the Hassid-Poreh One-Equation Energy Model, Letters in Heat and Mass Transfer, Vol. 5, pp. 73-80, 1978.
 - 44) Norris, L. H. and Reynolds, W. C. : Turbulent Channel Flow with a Moving Wavy Boundary, Rept. No. FM-10, Stanford University, Dept. Mech. Eng., Stanford, CA, 1975.
 - 45) Wolfshtein, M. : The Velocity and Temperature Distribution in One-Dimensional Flow with Turbulence Augmentation and Pressure Gradient, International Journal of Heat and Mass Transfer, Vol. 12, pp. 301-318, 1969.
 - 46) Hanjalic, K., Launder, B. E. and Schiestel, R. : Multiple-Time-Scale Concepts in Turbulent Transport Modeling, Turbulent Shear Flow, Vol. 2, edited by L. J. S. Bradbury, F. Durst, B. E. Launder, F. W. Schmidt, and J. H. Whitelaw, Springer-Verlag, Berlin, pp. 36-49, 1980.
 - 47) Wilcox, David C. : Multiscale Model for Turbulent Flows, AIAA Journal, Vol. 26, No. 11, pp. 1311-1320, Nov. 1988.
 - 48) Wilcox, David C. : Reassessment of the Scale Determining Equation for Advanced Turbulence Models, AIAA Journal, Vol. 26, No. 11, pp. 1299-1310, Nov. 1988.
 - 49) Frieche, C. A., van Atta, C. W. and Gibson, C. H. : AGARD Conference Proceedings, 93, 18. 1, 1971.
 - 50) Kolmogorov, A. N. : Dissipation of Energy in Locally Isotropic Turbulence, C. R. Acad. Sci. U. R. S. S., Vol. 32, p. 16, 1941.
 - 51) Mansour, N. N. and Shih, T. H. : Advancements in Turbulence Modeling, 3 rd ASCE/ASME Mechanics Conference, La Jolla, California, July 9-12, 1989, Forum on Turbulent Flows, ASME FED Vol. 76, pp. 129-141.
 - 52) Rogallo, R. S. : Numerical Experiments in Homogeneous Turbulence, NASA TM 81315, Ames Research Center, Moffet Field, CA, 1981.
 - 53) Rogallo, R. S. and Moin, P. : Numerical Simulation of Turbulent Flows, Ann. Review of Fluid Mechanics, pp. 99-137, 1984.
 - 54) Moser, R. D. and Moin, P. : Direct Numerical Simulation of Curved Turbulent Channel Flow, NASA TM 85974, NASA-Ames Research Center, Moffett Field, CA, 1984.
 - 55) Spalart, P. R. : Numerical Study of Sink-Flow Boundary Layers, J. Fluid Mech., Vol. 172, pp. 307-328, Nov. 1986.
 - 56) Spalart, P. R. : Direct Simulation of a Turbulent Boundary Layer up to $Re_\tau=1400$, J. Fluid Mech., Vol. 187, pp. 61-98, Feb. 1988.
 - 57) Lee, M. J. and Reynolds, W. C. : Numerical Experiments on the Structure of Homogeneous Turbulence, Report No. TF-24, Dept. of Mech. Eng., Stanford University, Stanford, CA, 1985.
 - 58) Rogers, M. M., Moin, P. and Reynolds, W. C. : The Structure and Modeling of the Hydrodynamic and Passive Scalar Fields in Homogeneous Turbulent Shear Flow, Report TF-24, Dept. of Mech. Eng., Stanford University, Stanford, CA, 1986.
 - 59) Mandelbrot, B. B. : How Long is the Coast of Britain? Statistical Self-Similarity and Fractional Dimension, Science, Vol. 156, pp. 636-638, 1967.
 - 60) Mandelbrot, B. B. : The Fractal Geometry of Nature, San Francisco, Freeman, 1982.
 - 61) Richardson, L. F. : Weather Prediction by Numerical Process, Cambridge University Press, 1922.
 - 62) Van Dyke, M. : An Album of Fluid Motion, Parabolic Press, Stanford, California, 1982.
 - 63) Chorin, A. J. : The Evolution of a Turbulent Vortex, Commun. Math. Phys., Vol. 83, pp. 517-535, 1982.

- 64) Sreenivasan, K.R. and Meneveau, C. : The Fractal Facets of Turbulence, *J. Fluid Mech.*, Vol. 173, pp.357-386, 1986.
- 65) Frisch, U., Sulem, P.L. and Nelkin, M. : A Simple Dynamical Model of Intermittent Fully Developed Turbulence, *J. Fluid Mech.*, Vol. 87, pp. 719-736, 1978.
- 66) Schertzer, D. and Lovejoy, S. : Physical Modeling and Analysis of Rain and Clouds by Anisotropic Scaling Multiplicative Processes, *J. Geophys. Res.*, 92 (D 8), pp.9693-9714, 1987.
- 67) Turcotte, D.L. : Annual review of Fluid Mechanics, Vol. 20, pp.5-16, 1988.
- 68) Ludwig, F.L. : Atmospheric Fractals—A Review, *Environmental Software*, Vol. 4, No. 1, pp.9-16, 1989.

(Received December 1 1989)
